

VIBRATIONAL RELAXATION TIMES  
OF GASEOUS MIXTURES OF DIATOMIC MOLECULES  
AND THEIR EFFECT ON ROCKET PERFORMANCE

Thesis by  
Harmon C. Penny  
Lieutenant, U. S. Navy

In Partial Fulfillment of the Requirements  
for the Degree of  
Aeronautical Engineer

California Institute of Technology  
Pasadena, California

1954

## ACKNOWLEDGEMENT

The author wishes to thank Dr. S. S. Penner for helpful discussion and Dr. Henry Aroeste for active assistance, instruction, and helpful criticism in the preparation of this thesis.

## SUMMARY

The present methods available for the determination of the magnitudes of the vibrational relaxation times of molecules are discussed and the recently developed theory of Schwartz, Slawsky, and Herzfeld is used to compute the variation with temperature of the collisional vibrational excitation probabilities of mixtures of  $\text{N}_2$  and  $\text{O}_2$ , and of  $\text{H}_2$  and HF. The results are used to estimate the extent of vibrational temperature lag in the hydrogen-fluorine rocket motor.

TABLE OF CONTENTS

<u>PART</u>	<u>TITLE</u>	<u>PAGE</u>
I.	INTRODUCTION	1
II.	EXPERIMENTAL METHODS	3
	A. THE SOUND VELOCITY METHOD	3
	B. IMPACT TUBE METHOD	5
	C. EXPERIMENTAL RESULTS	9
III.	THEORETICAL CALCULATIONS	10
IV.	VIBRATIONAL LAG IN THE HYDROGEN- FLUORINE ROCKET MOTOR	16

## I. INTRODUCTION

The internal energy,  $E$ , of a gas may be written, approximately, as the sum of energies of translation, rotation, vibration, and electronic motion. That is to say, we write that

$$E = E_{\text{trans}}(T) + E_{\text{rot}}(T_r) + E_{\text{vib}}(T_v) + E_{\text{el}}(T_e). \quad (1)$$

where  $T, T_r, T_v$ , and  $T_e$  represent, respectively, the absolute temperatures associated with the translational, rotational, vibrational, and electronic energy states. Under some conditions these energy states will be in equilibrium such that  $T = T_r = T_v = T_e$ . If, in the flow of a gas, temperature changes occur at rates sufficiently high to exceed the time required for these internal energy states to readjust themselves, the gas will depart from its equilibrium partition of energy.

The term "vibrational relaxation time" has come into use as a measure of the time required to establish equilibrium with respect to the internal vibrations of the molecules. The other internal states adjust themselves so rapidly that we can usually neglect their relaxation times. The vibrational relaxation time,  $\tau$ , is defined by the relation

$$dE_{\text{vib}}(T)/dt = \tau^{-1} [E_{\text{vib}}(T) - E_{\text{vib}}(T_v)]. \quad (2)$$

Working fluids such as steam, air, and exhaust gases have considerable vibrational heat capacity at high temperatures. If these gases have relaxation times comparable with or shorter than the intervals during which temperature changes occur in the gas, losses

must be expected. For turbine working fluids, Kantrowitz<sup>(1)</sup> estimates that in some cases the losses at high temperatures due to this adjustment lag can be comparable with the losses due to skin friction. Unfortunately, there exists a scarcity of data on the magnitudes of the relaxation times of most gases and, without these values being **known** at various temperature levels, their effects cannot be analyzed.

Various experimental methods have been devised to measure relaxation times of gases. Of these, only the two discussed here have been used with any degree of success. A third method involving a shock tube has been proposed, but has as yet not actually been used.

## II. EXPERIMENTAL METHODS

### A. THE SOUND VELOCITY METHOD<sup>(2)</sup>

The sound velocity method can be adapted for the determination of the relaxation times of gases up to temperatures of the order of 2300°K. The two essentials are (a) the production of sound waves of a definite frequency and (b) the accurate measurement of temperature.

The apparatus, originated by Pierce<sup>(3)</sup>, consists essentially of a carbon tube which can be heated to a high temperature and in which a stationary train of sound waves can be set up from a quartz crystal vibrating piezo-electrically. A piston traverses the tube. The position of the piston is read on an accurately graduated steel rule. This piston functions as a reflector to set up a standing wave system in the tube. The amplitude of vibration of the crystal changes as the reflector is moved along the tube. Resonance is detected by observing the magnitude of the plate current of the oscillator which maintains the quartz crystal in vibration. The half wave-length is determined by recording the different positions of the reflector at which resonance occurs. The temperature of the gas in the tube is measured by sighting an optical pyrometer of the "disappearing filament" type on to the face of the movable reflector. An electric furnace surrounds the carbon tube so that the temperature may be adjusted to higher levels. Figure 1 shows the general layout of the apparatus.

The velocity of sound,  $V$ , in the gas is computed from the measured half-wave length in the tube and from the known frequency

of vibration of the crystal. The ratio of specific heats is given by the formula,

$$\gamma = V^2 M / RT , \quad (3)$$

where M is the molecular weight, R is the gas constant, and T is the absolute temperature. The correction necessary to the above formula for departure from the perfect gas laws is negligible, since at the temperatures involved most gases are essentially perfect gases. From the observed data, an apparent ratio of specific heats, which we may call  $\gamma'$ , is computed from Eq. (3). Also from the relationship,

$$C_v / R = 1 / (\gamma - 1) , \quad (4)$$

an apparent specific heat at constant volume,  $C_v'$ , can be obtained.

The crystal used for the production of sound waves, if cut properly, can be made to vibrate in either the flexural mode or the longitudinal mode by suitable electronic circuitry. The two frequencies produced may vary by as much as 20,000 cps or more. The apparent specific heat obtained at each of these frequencies may differ considerably. Kneser<sup>(4)</sup> has put forth the following explanation for this phenomenon. As a sound wave of a given frequency passes through a gas, a part of the vibrational energy fails to follow the acoustic cycle, and the gas departs from its equilibrium condition. In fact, a part of the vibrational energy vanishes from the expression for the adiabatic elasticity, thus giving an increased



sound velocity. Kneser's theory led to the following formula for the apparent specific heat, derived from the velocity of sound data,

$$C_v = \frac{C_v^2 + 4\pi^2 n^2 \tau^2 C_d^2}{C_v + 4\pi^2 n^2 \tau^2 C_d} \quad , \quad (5)$$

where  $C_v$  = true specific heat

$n$  = frequency of the sound wave

$C_d$  = specific heat of translation and rotation (=  $5R/2$  for a diatomic molecule).

The values of the apparent specific heats may be substituted in this equation to give two equations at each temperature for the determination of  $\tau$  and  $C_v$ .

## B. IMPACT TUBE METHOD

In 1942 Kantrowitz<sup>(1)</sup> proposed the impact tube method for finding relaxation times and made sufficient measurements to verify that the experimental results checked with the theoretical calculations that were available at the time. Griffith<sup>(5)</sup> later extended this work and in 1950 reported on the results of his investigations, listing the relaxation times determined and expressing confidence in the method.

In the impact tube method, gas at rest is allowed to expand adiabatically through a nozzle, and the flow thus produced is brought to rest again by compression at the nose of an impact tube (pitot tube). The total head defect in the flow, as a measure of the entropy increase, is directly associated with the heat-capacity lag of the gas and can be used to determine the relaxation time. The process is shown schematically in Figure 2.

The underlying principles involved may be summarized briefly as follows. The equations of momentum, continuity, and energy for a compressible fluid with possible separate translational and vibrational temperatures, together with the standard definition for entropy, may be combined to establish the relationships,

$$ds = \left[ \frac{1}{T_{vib}} - \frac{1}{T} \right] d(C_{vib} T_{vib}), \quad (6)$$

$$\frac{d}{dt} (C_{vib} T_{vib} + C_p T + q^2/2) = 0. \quad (7)$$

The notation  $C_{vib}$  refers to the specific heat of vibrational motion. We have then that  $C_{vib} \equiv dE_{vib}/dT_{vib}$ , and if  $C'_p$  is the specific heat at constant pressure excluding contributions from vibration, we also have that  $C_p = C'_p + C_{vib}$ .

Using the theory of Landau and Teller<sup>(6)</sup>, the variation of  $C_{vib} T_{vib}$  with time may be expressed as

$$\frac{d}{dt} (C_{vib} T_{vib}) = C_{vib} (T - T_{vib}) / \tau; \quad (8)$$

on the basis of considerations involving molecular collisions, the relaxation time is found to have the following functional dependence:

$$\tau \approx p^{-1} (\nu s)^{-2/3} (m/T)^{-1/3} \exp \left[ (\nu s)^{2/3} (m/T)^{1/3} \right]. \quad (9)$$

The quantities  $\nu$ ,  $s$ , and  $m$  represent, respectively, vibrational frequency, molecular radius, and molecular mass.

The departure from equilibrium between vibrational and

translational temperatures was expressed by Kantrowitz as

$$\epsilon \equiv C_{vib}(T_{vib} - T). \quad (10)$$

In this experiment the changes in  $T$  are small compared to  $T$  itself, and Eq. (6) is reduced to

$$ds = \frac{\epsilon dt}{\tau} \frac{T - T_{vib}}{T T_{vib}} = \frac{\epsilon^2 dt}{\tau C_{vib} \bar{T}^2}. \quad (11)$$

$\bar{T}^2$  is taken as the average of  $T T_{vib}$  over the whole process.

The total head defect  $\Delta h$  is measured as the pressure difference  $p_0 - p_3$ , and since this difference is small compared to  $p_0$ , the differential change in entropy,  $ds = -Rdp/p$ , may be closely approximated by

$$\Delta S \approx \Delta h R / p_0. \quad (12)$$

Combining Eqs. (11) and (12) we obtain the relationship,

$$\Delta h / p_0 = \int \frac{\epsilon^2 dt}{R \tau C_{vib} \bar{T}^2}. \quad (13)$$

If the temperature is eliminated from Eqs. (7), (8), and (10), it is found that

$$\frac{d\epsilon}{dt} + \frac{C_p \epsilon}{C_p' \tau} = \frac{C_{vib}}{C_p'} \frac{d(q^2/2)}{dt}. \quad (14)$$

For the fast stopping compression process at the nose of the impact tube, the second term of this expression becomes small in comparison with the other terms, and the change in  $\epsilon$  becomes

$$\Delta \epsilon = \frac{C_{vib}}{C_p'} \frac{\Delta q^2}{2}. \quad (15)$$

Since at the beginning of compression  $\epsilon$  is zero and the velocity is  $q_1$ , Eq. (15) becomes

$$\epsilon_0 = \frac{C_{vib}}{C_p'} \frac{q_1^2}{2} . \quad (16)$$

With  $q = 0$ , Eq. (14) is reduced to

$$\frac{d\epsilon}{dt} = - \frac{C_p \epsilon}{C_p' \tau} . \quad (17)$$

For instantaneous compression the result is accordingly,

$$\frac{\Delta h_{ic}}{p_0} = \int_{\epsilon_0}^0 \frac{\epsilon^2 dt}{\tau R C_{vib} \bar{T}^2} = \frac{C_p'}{2 C_p R C_{vib} \bar{T}^2} \left( \frac{C_{vib} q_1^2}{2 C_p'} \right)^2 . \quad (18)$$

At this point it is convenient to introduce the following set of dimensionless parameters:

$$\begin{aligned} \tau' &= C_p' q_1 \tau / C_p d , & \epsilon' &= 2 C_p' \epsilon / C_{vib} q_1^2 , \\ t' &= q_1 t / d , & q' &= q / q_1 , \end{aligned} \quad (19)$$

where  $d$  is the diameter of the impact tube.

If Eqs. (13), (18), and (19) are now combined, it is found that

$$\frac{\Delta h}{\Delta h_{ic}} = \frac{2}{\tau'} \int \epsilon'^2 dt . \quad (20)$$

In order to determine the value of  $\epsilon'$  in this expression it is necessary to solve Eq. (14) exactly, the integral being

$$\epsilon = \exp \left[ - \int_{\tau_1}^{\tau} \frac{C_p dt}{\tau C_p'} \right] \int_{\tau_1}^{\tau} \exp \left[ \int_{\tau_1}^{\tau} \frac{C_p dt}{\tau dt} \right] \frac{C_{vib} d(\frac{q^2}{2})}{C_p' dt} dt , \quad (21)$$

which, stated in terms of the dimensionless parameters, leads to the expression

$$\epsilon' = \exp\left[-\frac{1}{\tau'} \int dt'\right] \int \exp\left[\frac{1}{\tau'} \int dt'\right] \frac{dq'^2}{dt'} dt'. \quad (22)$$

The integration of Eq. (22) has been done numerically for various values of  $\tau'$ . The integration of Eq. (20) has been carried out graphically, and from these resulting values a curve of  $\Delta h / \Delta h_{ic}$  vs.  $\tau'$  has been prepared. With this curve on hand an experiment may be conducted using any gas, and the relaxation time may be determined from the measured values of  $T_0$ ,  $p_0$ , and  $p_1$ . The values of  $C_{vib}$ ,  $C'_p$ ,  $C_p$ , and  $R$  for the gas can be found by the use of well-known statistical methods.

The procedure then is as follows.

- a) Calculate  $T_1$  from the relationship,  $T_1 = T_0 (p_1/p_0)^{R/C_p}$ .
- b) Calculate  $q_1$  from the relationship,  $q_1 = [2C_p(T_0 - T_1)]^{1/2}$ .
- c) Calculate  $\Delta h_{ic}$  from Eq. (18).
- d) Calculate  $\Delta h$  from the relationship,  $\Delta h = p_0 - p_1$ .
- e) Use the ratio of  $\Delta h / \Delta h_{ic}$  to enter into the graph of  $\Delta h / \Delta h_{ic}$  vs.  $\tau'$  to find the corresponding value for  $\tau'$ .
- f) Calculate the relaxation time,  $\tau$ , from the relationship,  $\tau = \tau' C_p d / C'_p q_1$ .

### C. EXPERIMENTAL RESULTS

Table I lists the values of the relaxation times of twenty gases determined experimentally by various investigators. The information in this table was obtained, for the most part, from Reference (5).

### III. THEORETICAL CALCULATIONS

The accumulation of a large body of experimental data led to efforts on the part of investigators to determine vibrational relaxation times using theoretical calculations. The method of Landau and Teller<sup>(6)</sup>, developed in 1936, and refined by Bethe and Teller<sup>(7)</sup> in 1940, has received general acceptance. A more detailed method developed by Schwartz, Slawsky, and Herzfeld<sup>(8,9)</sup> was published in 1952. This method of calculation is based on the fact that an equilibrium between the various degrees of freedom can be reached only by means of a transfer of energy taking place during a molecular collision. Thus for a pure gas it can be said that

$$\frac{1}{\tau} = M_{a,a} P, \quad (23)$$

where  $M_{a,a}$  is the number of collisions a molecule experiences per second and is proportional to the density, while  $P$  is the probability that upon a collision a quantum of vibrational energy will be converted to translational energy. For a gas composed of polyatomic molecules or mixtures of different types of molecules, there arises the possibility of an energy exchange between the different vibrational degrees of freedom during a collision as well as exchanges with the translational degrees of freedom, and a separate relaxation time must be ascribed to each of these energy transfers.

The theory of Schwartz, Slawsky, and Herzfeld will be used in this paper to compute the variation of vibrational excitation probabilities with temperature of mixtures of  $O_2$  and  $N_2$ , and of  $HF$  and  $H_2$ . For a mixture of molecules of type a and b, following the notation of

Schwartz et al, we may define the probabilities  $P_{0 \rightarrow 0}(a,a)$ ,  $P_{0 \rightarrow 0}(b,b)$ ,  $P_{0 \rightarrow 0}(a,b)$ ,  $P_{0 \rightarrow 0}(b,a)$ ,  $P_{0 \rightarrow 1}(a,b)$ ,  $P_{0 \rightarrow 1}(b,a)$ .

In each of these cases, the molecule, the symbol of which appears first in the parenthesis, was initially in the first excited vibrational state and finally in the ground or zeroth vibrational state. The subscript designates the behavior of the vibrational quantum number of the molecule, the symbol of which appears second in the parenthesis. Each of these probabilities has been tabulated and graphed as functions of temperature for both the  $O_2 - N_2$  and  $HF - H_2$  gaseous mixtures.

The probability  $P_{0 \rightarrow 1}(b,a)$  may be obtained from the relation

$$P_{0 \rightarrow 1}(b,a) = P_{0 \rightarrow 1}(a,b) e^{-h(\nu_a - \nu_b)/kT}. \quad (24)$$

The others are determined independently. These probabilities may then be used to obtain the relaxation times from the relations

$$\frac{1}{\tau(a,a)} = M_{a,a} P_{0 \rightarrow 0}(a,a) \left(1 - e^{-h\nu_a/kT}\right), \quad (25)$$

and

$$\frac{1}{\tau(a,b)} = M_{a,b} P_{0 \rightarrow 0}(a,b) \left(1 - e^{-h\nu_a/kT}\right). \quad (26)$$

Here  $M_{a,a}$  and  $M_{a,b}$  denote the number of collisions of the designated type per second. We may define similarly  $\tau(b,b)$  and  $\tau(b,a)$ .

For the complex excitation process it we may write

$$\frac{1}{\tau_{a,b}(a,b)} = X_a X_b M_{a,b} P_{0 \rightarrow 1}(a,b) \frac{1 - e^{-h\nu_a/kT}}{1 - e^{-h\nu_b/kT}}. \quad (27)$$

with a similar definition for  $\tau_{b,a}(b,a)$ . Here  $X_a$  and  $X_b$  are respectively the mole fractions of species a and species b in the mixture. It should be noted that only under special circumstances can the relaxation times defined above be grouped together to represent an effective relaxation time which corresponds to a measured relaxation time.

In general, we may write for the probabilities

$$P = CP', \quad (28)$$

where

$$P' = 1.18 \left( \frac{8\pi^2 \mu \Delta E}{\alpha^{*2} h^2} \right)^2 \sigma_i^{1/2} e^{-\sigma} \prod_i V^2(i), \quad (29)$$

$$C = 0.45 \left[ \left( 1 - \frac{\sigma_i kT}{3\epsilon} \right) + 1 \right]^{-1/3} e^{-\epsilon/kT}, \quad (30)$$

$$\sigma_i = \frac{3\mu v_0^{*2}}{2kT}, \quad (31)$$

$$\sigma = \frac{3\mu v_0^{*2}}{2kT} \pm \frac{\Delta E}{2kT}, \quad (32)$$

$$v_0^* = \left( \frac{4\pi^2 kT \Delta E}{\alpha^* h \mu} \right)^{1/3} \pm \frac{\Delta E}{2\mu} \left( \frac{4\pi^2 kT \Delta E}{\alpha^* h \mu} \right)^{-1/3} \quad (33)$$

and

$$\alpha^* = \frac{17.5}{r_0}. \quad (34)$$

Here  $\mu$  is the reduced mass of the two colliding molecules,  $\Delta E$  represents the amount of energy exchanged between vibration and translation,  $r_0$  and  $\epsilon$  are the usual constants in the Lennard-Jones interaction potential, and  $V(i)$  is the customary perturbation



integral over harmonic oscillator wave functions. For molecules whose value of  $\epsilon$  is not too great, it is sufficient to write

$\alpha^* = 17.5/r_0$ . In the case of HF, where sufficient virial coefficient, or transport data are not available, the collision diameter,  $r_0$ , was estimated by plotting  $r_0$  as a function of the electronegativity of the halogen atoms. From Fig. 3, it can be seen that the value of  $r_0$  for HF is approximately 1.7A.

The condition

$$\mu v_0^{*2}/2 > \Delta E \quad (35)$$

will not hold below a certain temperature for each of the probabilities. We need this inequality to write the expansion

$$v_f^* = v_0^* \pm \frac{\Delta E}{\mu v_0^*} - \frac{(\Delta E)^2}{2\mu^2 v_0^{*3}} + \dots \quad (36)$$

It is not necessary that

$$\mu v_0^{*2}/2 \gg \Delta E$$

although the larger the inequality, the better the convergence.

Schwartz and Herzfeld, in the appendix of their paper, have given a more complex method of computation which applies in the region of or below the limit temperatures defined by Eq. (35).

The following derivation applies for the determination of the temperature limit for which the basic equations used here will be applicable. The condition required by inequality (35) may be restated as

$$v_0^* > (2\Delta E/\mu)^{1/2}.$$

If we combine this expression with Eq. (33) we obtain

$$\left( \frac{4\pi^2 k T \Delta E}{\alpha^* h \mu} \right)^{1/3} - \frac{\Delta E}{2\mu} \left( \frac{4\pi^2 k T \Delta E}{\alpha^* h \mu} \right)^{-1/3} > \left( \frac{2\Delta E}{\mu} \right)^{1/2}. \quad (37)$$

If

$$\frac{4\pi^2 k \Delta E}{\alpha^* h \mu} = J, \text{ and } \left( \frac{2\Delta E}{\mu} \right)^{1/2} = B,$$

inequality (37) is reduced to

$$(JT)^{1/3} - B^2/4(JT)^{1/3} > B,$$

whence

$$J^{1/3} T^{2/3} - B T^{1/3} - B^2/4 J^{1/3} > 0. \quad (38)$$

We may obtain from this inequality the lower temperature limit of such that

$$T_{\text{limit}} = 1.758 B^3/J,$$

or

$$T_{\text{limit}} = \frac{1.24 \alpha^* h}{\pi^2} \left( \frac{\Delta E}{\mu} \right)^{1/2}. \quad (39)$$

Eq. (39) has been used to compute the values of the limit temperatures shown in Table II.

A compilation of the constants used in making the calculations indicated by the basic equations is shown in Table III. The constants in the Lennard-Jones interaction potential,  $\frac{\epsilon}{k}$  and  $r_0$ , were obtained from data listed in the "Transactions of the ASME"<sup>(10)</sup>, with the exception of the value for  $r_0$  for HF which was estimated in the manner already described. The vibrational constant  $\nu$  was found in each case from "Spectra of Diatomic Molecules" by Herzberg<sup>(11)</sup>.

The results of the indicated computations are listed in Table IV and shown graphically in Figures 4 and 5. The values indicated for the  $O_2 - N_2$  mixture agree within a few percent with those listed in the paper by Slawsky and Herzfeld. It is believed that where differences do exist, they may be attributed to a variation in the selection of force constants and low-velocity collision diameters inasmuch as the published values are not always consistent. The calculated relaxation times also agree reasonably well with values determined experimentally, as discussed in the paper of Schwartz et al. No data are available for comparison with our results for the  $HF - H_2$  probabilities.

#### IV. VIBRATIONAL LAG IN THE HYDROGEN-FLUORINE ROCKET MOTOR

It is now possible to present some brief considerations in determining whether or not the adiabatic expansion through the de Laval nozzle in the  $H_2 - F_2$  rocket motor may be taken as vibrational near-equilibrium flow. The reactants are taken in such proportion that  $H_2$  will be in excess, so that the products of combustion passing through the nozzle will be mostly a mixture of HF and  $H_2$ .

Following a procedure analogous to that of Penner<sup>(12)</sup>, in his treatment of chemical reaction in nozzle flow, we may take as an estimate for the vibrational temperature lag for near-equilibrium flow that

$$\Delta T \approx (DT/Dt) \tau \quad (40)$$

For representative nozzles in 1,000 psia thrust chambers, it has been found<sup>(13)</sup> that the cooling rate  $(-DT/Dt) \approx (T_c - T_e)/t_r \approx 3 \times 10^{-7}$  °K/sec. The use of very small nozzles will, of course, increase the cooling rate above this value; however, for nozzles in larger thrust engines,  $(-DT/Dt)$  will generally be less than  $3 \times 10^{-7}$  °K/sec, thereby leading to better approximations of near-equilibrium flow than we estimate below.

From Figure 5 it can be seen that the probability  $P_{0 \rightarrow 1}(a,b)$  is approximately as large as some of the other probabilities and much larger than others. The smaller probabilities contribute little to the effective relaxation time and may be neglected. The

probabilities, which are approximately as large as  $P_{0 \rightarrow 1}(a,b)$ , all contribute to the effective relaxation time. For the purpose of simplicity, however, it may be assumed that the maximum possible value of the effective relaxation time can be approximated as

$$\tau_m \approx \tau_{a,b} \approx 1 / X_a X_b M_{a,b} P_{0 \rightarrow 1}(a,b) . \quad (41)$$

The actual value of  $\tau$  must, of necessity, be smaller than  $\tau_m$  as the other probabilities, which are approximately as large as  $P_{0 \rightarrow 1}(a,b)$  have not been considered in computing  $\tau_m$  and would lower its value. If we can show, however, that vibrational near-equilibrium flow exists for the calculated upper limit,  $\tau_m$ , the conclusion will certainly hold for the real  $\tau$  which is smaller than  $\tau_m$ .

Since  $M_{a,b}$ , which denotes the number of collisions per second between HF and  $H_2$  molecules, increases markedly with pressure, it is apparent that if the conditions at the nozzle exit are such that vibrational near-equilibrium flow exists there, then it must also exist everywhere in the nozzle. The value of  $\Delta T$  was therefore computed at the nozzle exit, where it is a maximum.\*

In the present computations, the nozzle exit pressure was taken as one atmosphere. The product  $X_a X_b$  will generally lie between the comparatively narrow limits of 0.25 and 0.20, and will usually be about 0.23. The product of  $M_{a,b}$  and  $P_{0 \rightarrow 1}(a,b)$  will not vary appreciably from  $4 \times 10^7$  between the temperatures, 1400 to 3000° K. Therefore, for exit temperatures within this range,  $\tau_m \leq 1 \times 10^{-7}$  sec and, for  $(-DT/Dt) \leq 3 \times 10^7$  °K/sec,

-----  
\*For a more detailed description of iterative lag calculations during nozzle flow, see Reference (14).

$$\Delta T_m \leq 3^\circ K .$$

The estimate that over the length of the nozzle the vibrational temperature lag cannot exceed  $3^\circ K$  indicates that vibrational near-equilibrium flow occurs during expansion in a de Laval nozzle for representative hydrogen-fluorine rocket motors.

## REFERENCES

1. Kantrowitz, A.: "Heat Capacity Lag in Gas Dynamics", Journal of Chemical Physics, Vol. 14, p. 150, 1946.
2. Sheratt, G. G., and Griffiths, E.: "The Determination of the Specific Heat of Gases at High Temperatures by the Sound Velocity Method", Proceedings of the Royal Society of London, Vol. 147A, p. 292, 1934.
3. Pierce, G. W.: "Piezoelectric Crystal Oscillators Applied to the Precision Measurement of the Velocity of Sound in Air and CO<sub>2</sub> at High Frequencies", Proceedings of the American Academy of Arts and Sciences, Vol. 60, p. 271, 1925.
4. Kneser, H. O.: "Zur Dispersionstheorie des Schalles", Annalen der Physik, Vol. 11, p. 761, 1931.
5. Griffith, W.: "Vibrational Relaxation Times in Gases", Journal of Applied Physics, Vol. 21, p. 1319, 1950.
6. Landau, L., and Teller, E.: "Zur Theorie der Schalldispersion", Physikalische Zeitschrift der Sowjetunion, Vol. 10, p. 34, 1936.
7. Bethe, H. A., and Teller, E.: "Deviations from Thermal Equilibrium in Shock Waves", Report X-117, Ballistics Research Laboratory, Aberdeen Proving Ground.
8. Schwartz, R., Slawsky, Z., and Herzfeld, K.: "Calculation of Vibrational Relaxation Times in Gases", Journal of Chemical Physics, Vol. 20, p. 1591, 1952.
9. Schwartz, R., and Herzfeld, K.: "Vibrational Relaxation Times in Gases (Three Dimensional Treatment)", Journal of Chemical Physics, Vol. 22, p. 8768, 1954.
10. Hirshfelder, J. O., Bird, R. B., and Spotz, E. L.: "Viscosity and Other Physical Properties of Gases and Gas Mixtures", 1949 Transactions of the American Society of Mechanical Engineers, Vol. 71, p. 921, 1949.
11. Herzberg, G.: Spectra of Diatomic Molecules, Table 39, p. 501.
12. Penner, S. S.: "Thermodynamics and Chemical Kinetics of One-dimensional Non-viscous Flow through a Laval Nozzle", Journal of Chemical Physics, Vol. 19, p. 877, 1951.
13. Altman, D., and Penner, S. S.: "Chemical Reaction During Adiabatic Flow through a Rocket Nozzle", Journal of Chemical Physics, Vol. 17, p. 56, 1949.
14. Penner, S. S.: "Linearization Procedures of the Study of Chemical Reactions Flow Systems", 1953 Iowa Thermodynamics Symposium.

Gas	$T$ $^{\circ}\text{K}$	$\tau \times 10^{-6}$ secs
<u>A. Sonic Velocity Method</u>		
Hydrogen	298	0.018 (rot)
Oxygen	294	1000
Carbon monoxide	1257	10
Chlorine	294	18
Carbon dioxide	294	10.8
Sulfur dioxide	294	0.181
Ammonia	294	0.04
Ethylene	294	0.238
Methane	383	0.84
Carbon disulfide	294	0.70
Nitrous oxide	292	0.92
<u>B. Impact Tube Method</u>		
Hydrogen	287	0.021 (rot)
Nitrogen	289	0.002
Nitrous oxide	291	1.12
Carbon dioxide (comm)	291	2.02
Sulfur dioxide	293	0.37
Ammonia	290	0.12
Methyl chloride	295	0.202
Ethane	287	0.003
Ethylene	289	0.207
Propylene	294	0.006
Propane	294	0.007
Ethylene oxide	303	1.23
Butane	294	0.018
Butadiene	294	0.013
Methane	289	0.48

TABLE I. Experimental results reported in Reference 5  
for the relaxation times of gases.



Probability	Temp °K	
	O <sub>2</sub> - N <sub>2</sub>	HF - H <sub>2</sub>
$P_{0 \rightarrow 0}(a,a)$	326°	1390°
$P_{0 \rightarrow 0}(b,b)$	405°	2700°
$P_{0 \rightarrow 0}(a,b)$	330°	2380°
$P_{0 \rightarrow 0}(b,a)$	403°	2440°
$P_{0 \rightarrow 1}(a,b)$	231°	592°
$P_{0 \rightarrow 1}(b,a)$	231°	592°

TABLE II. Lower temperature limits for which the probabilities can be calculated from the theory of Schwartz, Slawsky, and Herzfeld.

O<sub>2</sub> - N<sub>2</sub>

°K	$P_{0 \rightarrow 0}(a,a)$	$P_{0 \rightarrow 0}(b,b)$	$P_{0 \rightarrow 0}(a,b)$	$P_{0 \rightarrow 0}(b,a)$	$P_{0 \rightarrow 1}(a,b)$	$P_{0 \rightarrow 1}(b,a)$
400	$8.8 \times 10^{-8}$	$3.3 \times 10^{-10}$	$9.0 \times 10^{-8}$	$7.1 \times 10^{-10}$	$9.5 \times 10^{-8}$	$1.6 \times 10^{-6}$
600	$6.8 \times 10^{-7}$	$3.6 \times 10^{-9}$	$6.1 \times 10^{-7}$	$5.7 \times 10^{-9}$	$1.0 \times 10^{-6}$	$6.9 \times 10^{-6}$
1000	$8.3 \times 10^{-6}$	$7.5 \times 10^{-8}$	$7.7 \times 10^{-6}$	$1.1 \times 10^{-7}$	$8.2 \times 10^{-6}$	$3.5 \times 10^{-5}$
1500	$5.5 \times 10^{-5}$	$7.2 \times 10^{-7}$	$5.1 \times 10^{-5}$	$1.2 \times 10^{-6}$	$5.6 \times 10^{-5}$	$1.2 \times 10^{-4}$
2000	$2.0 \times 10^{-4}$	$3.9 \times 10^{-6}$	$1.9 \times 10^{-4}$	$4.8 \times 10^{-6}$	$1.6 \times 10^{-4}$	$2.8 \times 10^{-4}$
2500	$5.2 \times 10^{-4}$	$1.3 \times 10^{-5}$	$4.9 \times 10^{-4}$	$1.7 \times 10^{-5}$	$3.1 \times 10^{-4}$	$4.8 \times 10^{-4}$
3000	$1.0 \times 10^{-3}$	$3.4 \times 10^{-5}$	$9.0 \times 10^{-4}$	$4.5 \times 10^{-5}$	$5.3 \times 10^{-4}$	$7.7 \times 10^{-4}$

HF - H<sub>2</sub>

1000	-	-	-	-	$1.1 \times 10^{-2}$	$1.6 \times 10^{-2}$
1500	$7.9 \times 10^{-5}$	-	-	-	$1.6 \times 10^{-2}$	$2.1 \times 10^{-2}$
2000	$1.9 \times 10^{-4}$	-	-	-	$1.9 \times 10^{-2}$	$2.3 \times 10^{-2}$
2500	$3.6 \times 10^{-4}$	-	$1.6 \times 10^{-3}$	$2.3 \times 10^{-2}$	$2.2 \times 10^{-2}$	$2.6 \times 10^{-2}$
3000	$6.1 \times 10^{-4}$	$2.1 \times 10^{-2}$	$2.2 \times 10^{-3}$	$3.3 \times 10^{-2}$	$2.5 \times 10^{-2}$	$2.8 \times 10^{-2}$

TABLE IV. Variation of probabilities with temperature

Probability	$r_0$ Å	$\epsilon/k$ °K	$\nu \times 10^{13}$ sec <sup>-1</sup>	$\Delta E \times 10^{-13}$ ergs
<u>O<sub>2</sub> - N<sub>2</sub></u>				
$P_{0 \rightarrow 0}(a,a)$	3.50	114.0	4.75	3.14
$P_{0 \rightarrow 0}(b,b)$	3.69	93.7	7.10	4.70
$P_{0 \rightarrow 0}(a,b)$	3.60	103.5	4.75	3.14
$P_{0 \rightarrow 0}(b,a)$	3.60	103.5	7.10	4.70
$P_{0 \rightarrow 1}(b,a)$	3.60	103.5	4.75 7.10	1.56
<u>HF - H<sub>2</sub></u>				
$P_{0 \rightarrow 0}(a,a)$	1.70	378.0	12.4	8.22
$P_{0 \rightarrow 0}(b,b)$	2.94	35.1	13.2	8.74
$P_{0 \rightarrow 0}(d,b)$	2.32	114.0	12.4	8.22
$P_{0 \rightarrow 0}(b,a)$	2.32	114.0	13.2	8.74
$P_{0 \rightarrow 1}(b,a)$	2.32	114.0	12.4 13.2	.52

TABLE III. Values of constants used in computations for the vibrational excitation probabilities.

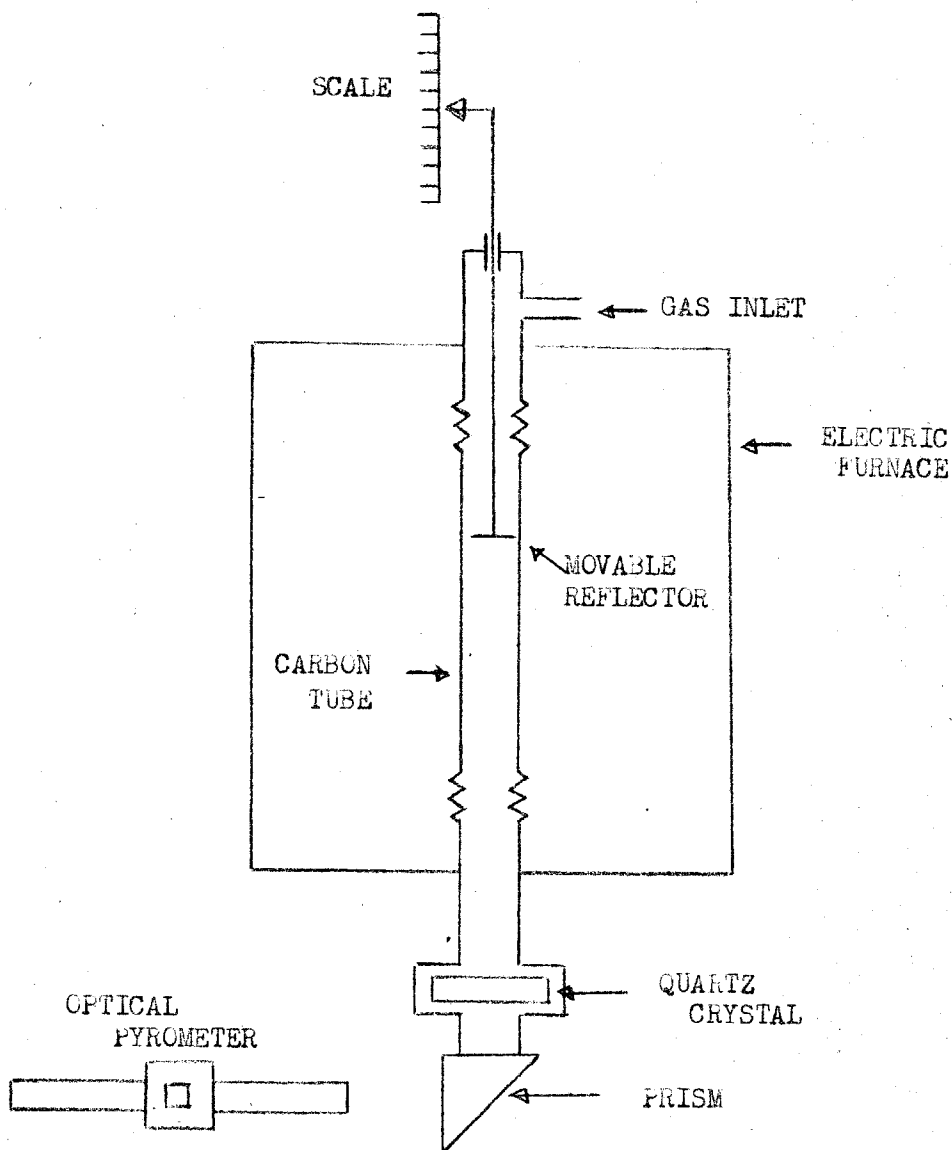


Fig. 1. Schematic drawing of apparatus for determining vibrational relaxation time by the sound velocity method.

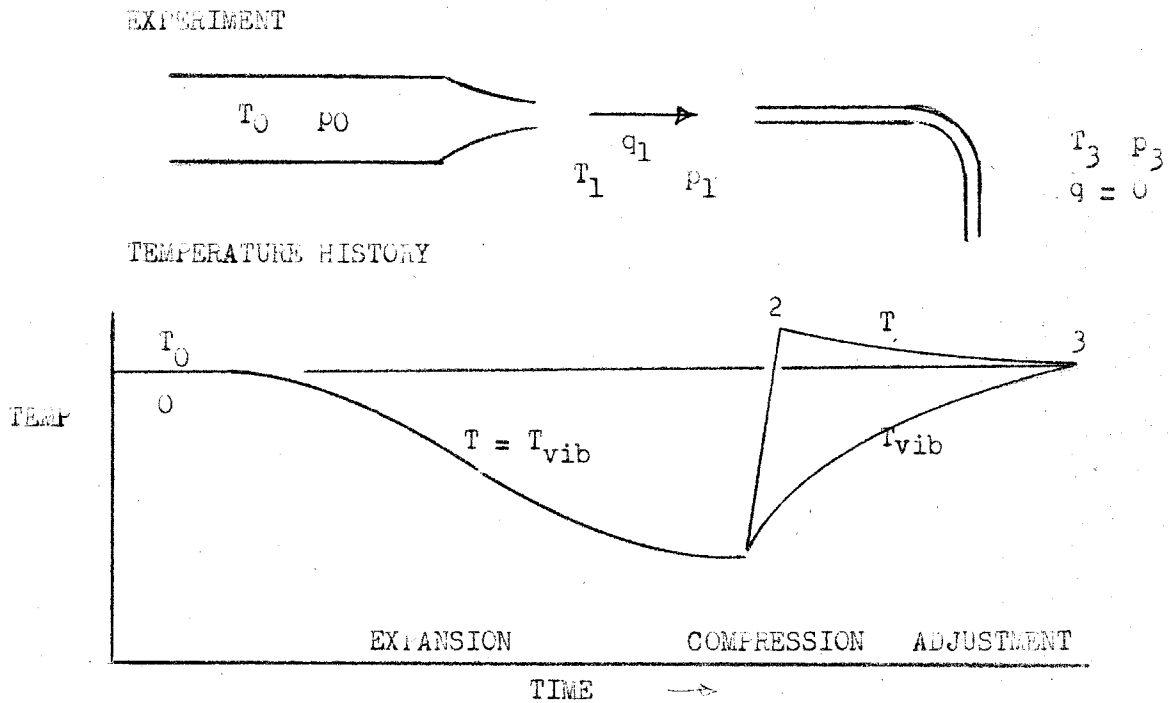


Fig. 2. Schematic drawing of the experiment and temperature history of the gas for determining vibrational relaxation time by the impact tube method.

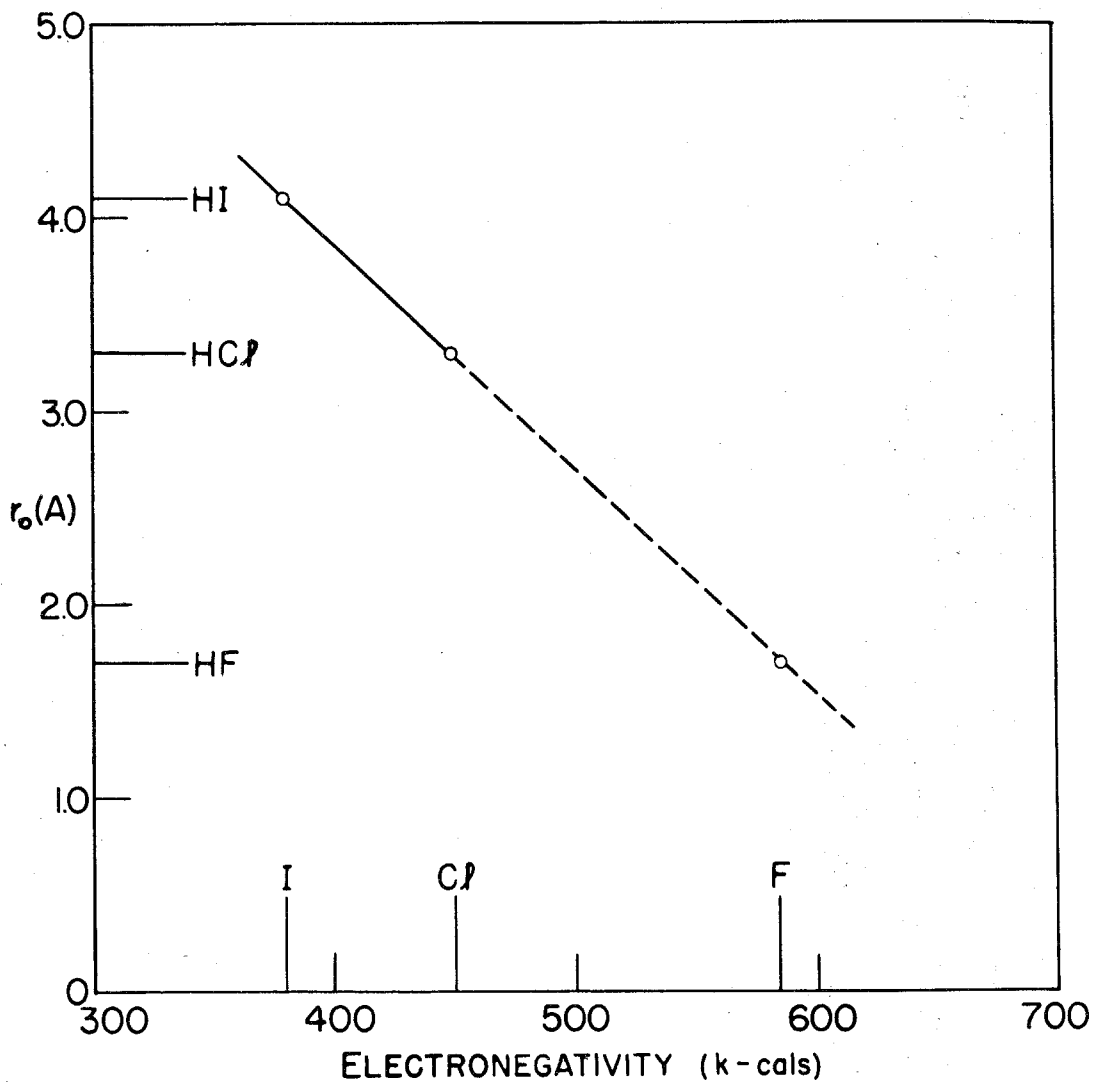


FIGURE 3- COLLISION DIAMETER AS A FUNCTION OF ELECTRONEGATIVITY.

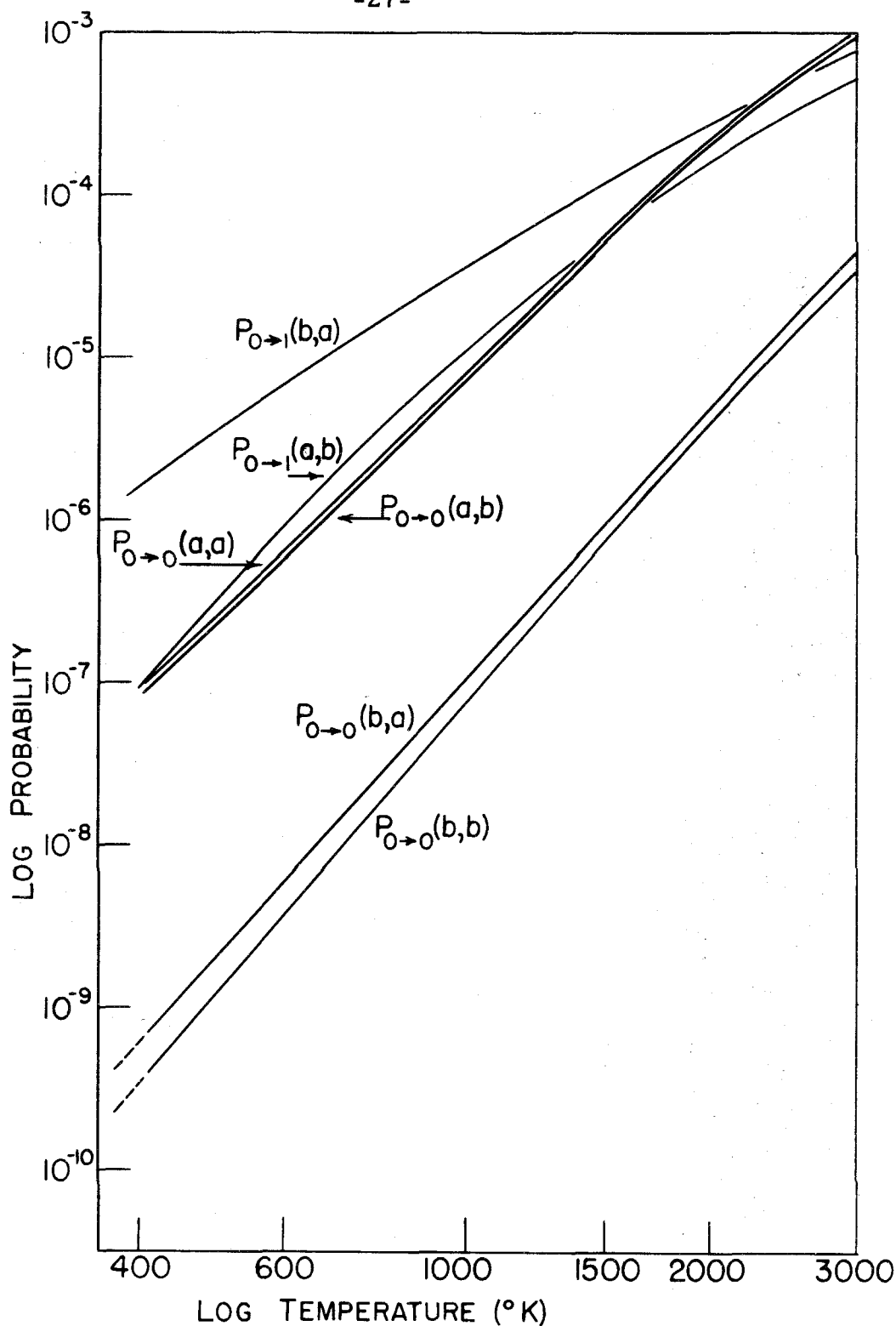


FIGURE 4- VARIATION OF ( $a = O_2, b = N_2$ ) PROBABILITIES WITH TEMPERATURE. LIMIT TEMPERATURES CORRESPOND TO THE JUNCTION BETWEEN THE SOLID PORTION AND THE DOTTED PORTION OF THE CURVES.

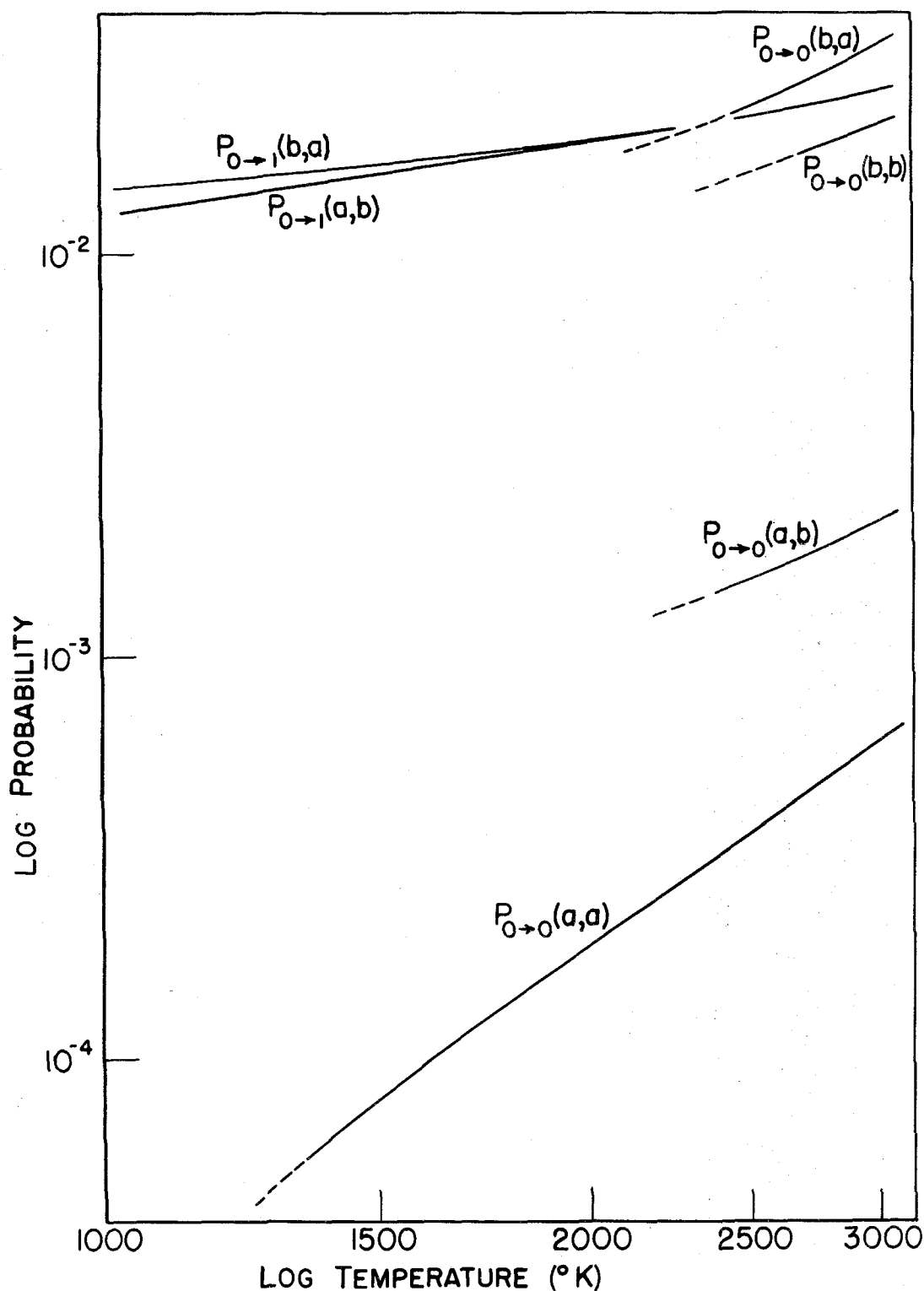


FIGURE 5- VARIATION OF ( $a = \text{HF}$ ,  $b = \text{H}_2$ ) PROBABILITIES WITH TEMPERATURE. LIMIT TEMPERATURES CORRESPOND TO THE JUNCTION BETWEEN THE SOLID PORTION AND THE DOTTED PORTION OF THE CURVES.